

## DYNAMICS OF THE IMPROVED BODY-CENTRED CUBIC LATTICE MODEL FOR POLYMER CHAINS\*

ZHANG LINXI† and XU JIANMIN

Department of Physics, Hangzhou University, Hangzhou, People's Republic of China

(Received 15 November 1989; received for publication 6 April 1990)

**Abstract**—We introduce the parameter of probability of movement and study the dynamics of polymer chains by using the improved body-centred cubic lattice model. The model can approach to simulate the dynamics of real polymer chains. We find that the relaxation times obey the relation  $T_R(P) \sim (N-1)^{2.05}/P^{0.75}$  in the absence of excluded volume and the relation  $T_R(P) \sim (N-1)^{2.33}/P^{0.95}$  in the presence of excluded volume, also the relation  $T_k(P) \sim T_k(1)/P^{\beta_k}$  ( $\beta_1 = \beta_2 = 0.77$ ,  $\beta_3 = 0.90$ ) in the absence of excluded volume. Comparisons with theoretical predictions are made.

### INTRODUCTION

Study of the dynamics of the lattice model for polymer chains using Monte Carlo techniques was initiated long ago by Verdier and Stockmayer [1]. The technique has been developed and applied to new problems primarily by Kranbuehl and Verdier [2]. The original work on isolated simple cubic (SC) lattice chains [3] confirms that, in the absence of excluded volume, the model shows essentially Rouse-like [4] behaviour in both the chain length,  $N$ , and mode number,  $k$ , dependence of the relaxation times. In the presence of excluded volume, a deviation from Rouse-like behaviour is seen in both  $N$  and  $k$  dependence. Later, Geny and Monnerie developed a tetrahedral lattice model [5] and Downy, Crabb and Kovac developed a body-centred cubic (BCC) lattice model [6] and a face-centred cubic (FCC) lattice model [7] to study the dynamics of polymer chains.

The cubic lattice model, however, requires two type of elementary motions, the two-bond "normal bead" motion and the three-bond "90° crankshaft", in order to create the proper dynamical algorithm; the tetrahedral lattice model also requires two types of elementary motions: the three-bond motion and the four-bond motion. However, the FCC lattice and BCC lattice models require only two-bond motion to create the proper algorithm. The FCC and BCC models gave results that were slightly closer than the SC model both the Rouse model in the absence of excluded volume and the dynamic scaling prediction in the presence of excluded volume. In the excluded volume case, the FCC model and BCC models also show a  $k$  dependence similar to that of the SC model.

In the study of both the chains length and mode number dependence of the dynamics of lattice models for polymer chains, it was thought that every bead moves on every occasion when the condition permits movement. In fact, every bead does not move at every occasion because of the effect of other beads on it. We

know that polymer chains move quickly at high temperature and slowly at low temperature, so it is necessary to introduce the parameter  $P$  of the probability of movement of polymer chains in the study of the dynamics of the lattice model for polymer chains. The parameter  $P$  is the probability of movement of polymer chains and depends on condition, temperature and interaction of polymer chains. Polymer chains move quickly for large  $P$  ( $P \leq 1$ ) and slowly for small  $P$ .

In our simulation, the polymer chain is modeled as a random walk of  $(N-1)$  steps of unit length on the BCC lattice. Each step is referred to as a bond. The chain occupies  $N$  lattice junctions, each of which is called a bead. A representative chain conformation is shown in Fig. 1. The chain moves according to the algorithm, which is similar to the algorithm for the SC lattice model [3, 8], BCC lattice model [6] and FCC lattice model [7] except for whether a bead moves or not according to the probability of movement  $P$ . The elementary time unit is taken to be  $N$  bead cycles. As the simulations proceeded, the end-to-end vector  $\vec{R}(t)$  was sampled at intervals, and the samples used to form estimates of the ensemble averages  $\langle \vec{R}(0) \cdot \vec{R}(t) \rangle$  as previously described [1]. The autocorrelation functions  $\rho_R(t)$  were defined by

$$\rho_R(t) = \langle \vec{R}(0) \cdot \vec{R}(t) \rangle / \langle R^2 \rangle, \quad (1)$$

where the broken brackets represent an equilibrium ensemble average. The equilibrium average was computed as a time average over a trajectory begun from a fully equilibrated chain conformation. The relaxation time  $T_R$  was estimated by fitting a least-squares line to the linear long-time region of a semilog plot of  $\rho_R(t)$  vs time. The inverse of the relaxation time is the negative of the slope of the line.

To analyse the dynamics in more detail, we also studied the relaxation of the first three normal modes. The normal modes  $\vec{U}_k(t)$  are given by the Rouse formula [9]

$$\vec{U}_k(t) = \sum_{j=1}^N [(2 - \delta_{k0})/N] \cos[(j - 1/2)\pi k/N] \vec{R}_j(t), \quad (2)$$

\*Project supported by the Science Fund of Zhejiang Province.

†To whom all correspondence should be addressed.

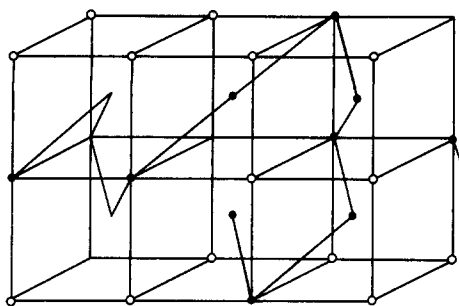


Fig. 1. Representative conformation of a BCC lattice polymer chain.

where  $\hat{R}_j(t)$  is the position of the  $j$ -th bead with respect to the origin. The Rouse coordinates have proved to form an excellent set of normal coordinates for the SC, FCC and BCC models. The autocorrelation function of the  $k$ -th normal mode,  $\rho_k(t)$ , is given by

$$\rho_k(t) = \langle \hat{U}_k(t) \cdot \hat{U}_k(0) \rangle / \langle U_k^2 \rangle. \quad (3)$$

The equilibrium ensemble average was again computed as a time average. The relaxation time of the  $k$ -th mode  $\rho_k(t)$  is computed by fitting a least-squares line to the semilog plot of  $\rho_k(t)$  vs time. The negative of the relaxation time is the inverse of the slope of this line.

## RESULTS

Simulations were carried out for chains of 15, 30, 45 and 60 beads with and without excluded volume. For all cases, simulations were carried out at four values of the probability of movement  $P$ , from 0.375

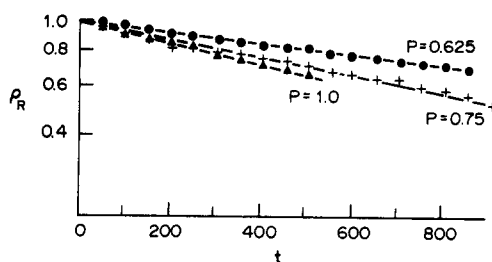


Fig. 2. Semilogarithmic plots of the normal coordinate autocorrelation function  $\rho_R(t)$  vs  $t$  for a chain of length  $N = 45$  and probability of movement  $P = 1.00, 0.75$  and  $0.625$  in the absence of excluded volume.

to 1.00. At least four runs for each chain with different values of  $P$  were done. Figure 2 shows end-to-end vector autocorrelation  $\rho_R(t)$  for  $N = 45$ , and  $P = 1.00, 0.75$  and  $0.625$ . It is clear from these semilog plots that the autocorrelation function is a single exponential at long times. The relaxation times  $T_R$  extracted from the long-time slope of the  $\ln \rho_R(t)$  vs  $t$  plot are collected in Table 1. In this table, the relaxation times  $T_R$  for  $P = 1.00$  agree well with Downey's results and we plot  $\ln T_R(1)$  vs  $\ln(N - 1)$ .  $T_R(1)$  may be written in the form

$$T_R(1) \sim (N - 1)\alpha_R. \quad (4)$$

In the absence of excluded volume, the value of  $\alpha_R$  is 2.05, which is essentially the same as the Rouse value of 2.0 and agrees with the value of 1.96 of Downey. In the presence of excluded volume, the value of  $\alpha_R$  is 2.33, which is quite close to the scaling theory prediction of 2.20 and agrees with the value of 2.27 of Downey. In Table 2, we calculate the ratio

Table 1. End-to-end vector relaxation times,  $T_R(P)$ , as a function of chain length,  $N$ , and probability of movement,  $P$

$P$	$T_R(P)$							
	No excluded volume				Excluded volume			
	$N = 15$	$N = 30$	$N = 45$	$N = 60$	$N = 15$	$N = 30$	$N = 45$	$N = 60$
1.00	24.5	117	271	538	69.3	375	1151	2190
0.75	31.5	153	340	682	86.2	470	1385	2697
0.625	35.6	185	408	789	109	578	1806	3398
0.375	50.0	241	565	1056	187	989	2820	5379

Table 2. The ratio  $T_R(P)/T_R(1)$  as a function of chain length,  $N$ , and probability of movement,  $P$

$P$	$T_R(P)/T_R(1)$							
	No excluded volume				Excluded volume			
	$N = 15$	$N = 30$	$N = 45$	$N = 60$	$N = 15$	$N = 30$	$N = 45$	$N = 60$
0.70	1.29	1.31	1.26	1.27	1.24	1.25	1.20	1.23
0.625	1.45	1.58	1.51	1.47	1.57	1.54	1.57	1.55
0.375	2.06	2.06	2.08	1.96	2.70	2.64	2.45	2.46

Table 3. Values of  $(N - 1)^{2.05}/[T_R(P)P^{0.75}]$  (no excluded volume) and  $(N - 1)^{2.33}/[T_R(P)P_{0.95}]$  (no excluded volume) as a function of chain length,  $N$ , and probability of movement,  $P$

$P$	$(N - 1)^{2.05}/[T_R(P)P^{0.75}]$				$(N - 1)^{2.33}/[T_R(P)P]$			
	No excluded volume				Excluded volume			
	$N = 15$	$N = 30$	$N = 45$	$N = 60$	$N = 15$	$N = 30$	$N = 45$	$N = 60$
1.00	9.13	8.51	8.63	7.93	6.76	6.81	5.86	6.10
0.75	8.81	9.13	8.94	7.76	7.14	7.14	6.40	6.50
0.625	8.94	7.69	8.16	7.69	6.71	6.89	5.87	6.16
0.375	9.24	8.62	8.64	8.43	6.36	6.56	6.10	6.31

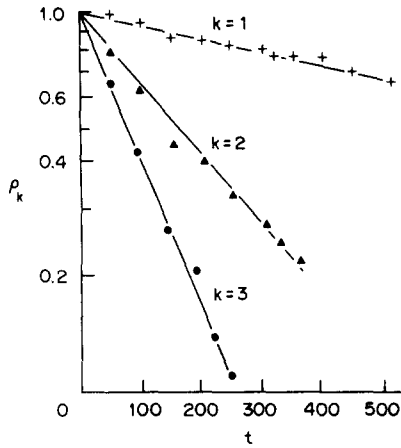


Fig. 3. Semilogarithmic plots of the normal coordinate autocorrelation function  $\rho_k(t)$  vs  $t$  for a chain of length  $N=45$  and a probability of movement  $P=1.00$  in the absence of excluded volume.

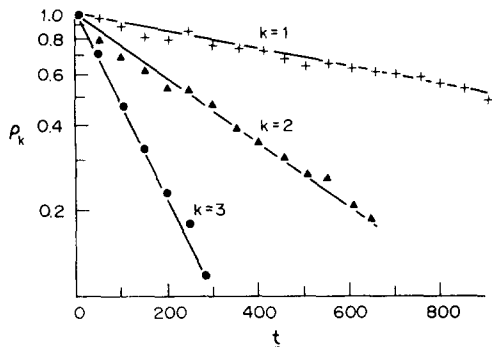


Fig. 4. Semilogarithmic plots of the normal coordinate autocorrelation function  $\rho_k(t)$  vs  $t$  for a chain of length  $N=45$  and a probability of movement  $P=0.75$  in the absence of excluded volume.

$T_R(P)/T_R(1)$ , and find that the ratio is almost independent of  $N$ , and may be written

$$T_R(P)/T_R(1) \sim P - \beta_R. \quad (5)$$

In the absence of excluded volume, the value of  $\beta_R$  is 0.75 and in the presence of excluded volume

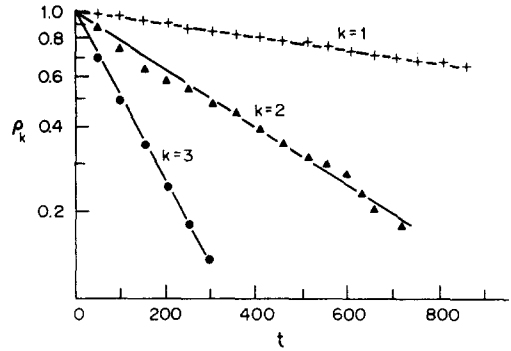


Fig. 5. Semilogarithmic plots of the normal coordinate autocorrelation function  $\rho_k(t)$  vs  $t$  for a chain of length  $N=45$  and a probability of movement  $P=0.625$  in the absence of excluded volume.

its value is 0.95. We also calculated the ratio  $(N-1)^{2.05}/[T_R(P)P^{0.75}]$  (without excluded volume) and the ratio  $(N-1)^{2.33}/[T_R(P)P^{0.95}]$  (with excluded volume) and the results are given in Table 3.

Figures 3–5 show representative semilog plots of the normal-mode autocorrelation function  $\rho_k(t)$  for the first three modes for a chain with different  $P$  without excluded volume. The semilog plots are linear. The relaxation times,  $\rho_k$ , obtained from the least-squares slopes of the  $\ln \rho_k(t)$  vs  $t$  plots, are collected in Table 4. We first discuss the  $T_k(1)$ , which previous authors have studied. We plot  $\ln T_k(1)$  vs  $\ln(N-1)$  at constant  $k$  and  $\ln T_k(1)$  vs  $\ln(k)$  at constant. We obtain

$$T_k(1) \sim (N-1)^{\alpha_k}, \quad (6)$$

$$T_k(1) \sim k^{-\gamma_N}. \quad (7)$$

The values of  $\alpha_k$  and  $\gamma_N$  are 2.00 and 1.94 respectively in the absence of excluded volume and are 2.20 and 2.12 respectively in the presence of excluded volume. All of the results agree well with the values of Rouse and Downey. In Table 4,  $T_k(P)$  for small  $P$  is greater than that for large  $P$ . In order to discuss the relation with  $P$ , we calculate the ratio  $T_k(P)/T_k(1)$  and the results are given in Table 5. We find that the ratio

Table 4. Normal co-ordinate relaxation times,  $T_k$ , as a function of chain length,  $N$ , and probability of movement,  $P$

$P$	$k$	$T_k(P)$							
		No excluded volume				Excluded volume			
		$N=15$	$N=30$	$N=45$	$N=60$	$N=15$	$N=30$	$N=45$	$N=60$
1.00	1	25.6	110	279	490	80.0	416	1150	2184
	2	6.4	31.8	72.3	129	19.2	90.1	244	532
	3	3.5	15.9	34.9	60.4	7.8	36.4	100	213
0.75	1	31.3	130	344	600	88.6	473	1370	2467
	2	7.6	45.1	94.0	148	23.4	112	380	685
	3	4.8	21.4	46.7	83.1	9.4	50.5	132	296
0.625	1	35.5	165	409	700	110	575	1735	3360
	2	8.7	48.7	101	181	35.1	150	423	959
	3	5.7	26.6	55.8	99.8	14.1	75.0	195	434
0.375	1	49.5	237	584	1000	188	1033	2720	5375
	2	13.3	68.5	150	272	50.0	226	682	1427
	3	7.9	36.8	76.8	137	29.0	147	421	969

Table 5. The ratio  $T_k(P)/T_k(1)$  as a function of chain length,  $N$ , and probability of movement,  $P$ 

$P$	$k$	$T_k(P)/T_k(1)$							
		No excluded volume				Excluded volume			
		$N = 15$	$N = 30$	$N = 45$	$N = 60$	$N = 15$	$N = 30$	$N = 45$	$N = 60$
0.75	1	1.22	1.19	1.23	1.22	1.11	1.15	1.19	1.13
	2	1.19	1.41	1.30	1.16	1.22	1.24	1.55	1.29
	3	1.37	1.35	1.34	1.39	1.20	1.39	1.32	1.29
0.625	1	1.39	1.50	1.47	1.42	1.38	1.40	1.51	1.54
	2	1.36	1.53	1.40	1.40	1.83	1.67	1.73	1.80
	3	1.63	1.67	1.60	1.66	1.81	2.06	1.95	1.89
0.375	1	1.93	2.15	2.09	2.20	2.35	2.52	2.37	2.46
	2	2.08	2.15	2.07	2.12	2.60	2.51	2.80	2.69
	3	2.20	2.31	2.20	2.28	3.72	4.00	4.21	4.21

Table 6. Values of  $P^{\beta_k} T_k(P)/T_k(1)$  ( $\beta_1 = \beta_2 = 0.77$ ,  $\beta_3 = 0.90$ ) (no excluded volume) as a function of chain,  $N$ , and probability of movement,  $P$ 

$P$	$k$	$P^{\beta_k} \cdot T_k(P)/T_k(1)$ ( $\beta_1 = \beta_2 = 0.77$ , $\beta_3 = 0.90$ )			
		$N = 15$	$N = 30$	$N = 45$	$N = 60$
0.75	1	0.98	0.95	0.99	0.98
	2	0.95	1.13	1.04	0.93
	3	1.05	1.04	1.03	1.07
0.625	1	0.97	1.04	1.02	1.00
	2	1.06	1.06	0.98	0.98
	3	1.07	1.09	1.05	1.08
0.375	1	0.91	1.01	0.98	1.03
	2	0.98	1.01	0.97	1.00
	3	0.91	0.96	0.91	0.94

$T_k(P)/T_k(1)$  is independent of  $N$  in the absence of excluded volume. We obtain

$$T_k(P)/T_k(1) \sim P^{-\beta_k}, \quad (8)$$

where  $\beta_1 = \beta_2 = 0.77$  and  $\beta_3 = 0.90$ . In Table 6 we calculate the ratio  $T_k(P)/[P^{\beta_k} \cdot T_k(1)]$  in the absence of excluded volume.

## CONCLUSIONS

Introducing the parameter  $P$  of probability of movement, we find that the relaxation times of polymer chains depend on solvent, temperature and interaction of polymer chains. In the meantime, we can simulate the dynamics of the real polymer chain by using Monte Carlo simulation.

## REFERENCES

1. P. H. Verdier and W. H. Stockmayer. *J. chem. Phys.* **36**, 227 (1962).
2. D. E. Kranbuehn and P. H. Verdier. *J. chem. Phys.* **71**, 2662 (1979).
3. M. Dial, K. S. Crabb, C. C. Crabb and J. Kovac. *Macromolecules* **18**, 2215 (1985).
4. P. E. Rouse. *J. chem. Phys.* **21**, 1273 (1953).
5. F. Geny and L. Monnerie. *J. Polym. Sci.; Polym. Phys. Edn* **17**, 131 (1979).
6. J. P. Downey and J. Kovac. *Macromolecules* **20**, 1357 (1987).
7. J. P. Downey, C. C. Crabb and J. Kovac. *Macromolecules* **19**, 2202 (1986).
8. C. C. Crabb and J. Kovac. *Macromolecules* **18**, 1430 (1985).
9. P. H. Verdier. *J. chem. Phys.* **45**, 2118 (1966).